ON A CONTROLLED COMPOSITE SEMI-INFINITE STRIP

Cristian RUGINĂ, Veturia CHIROIU, Ligia MUNTEANU

The configuration for a semi-infinite strip with self tuning based control is presented in this paper. The semi-infinite strip is composed from a layer of main material, and another layer of piezoelectric material with Cantor-like structure. We show that the displacements distribution can be controlled actively by applying a voltage to the piezoelectric material.

1. INTRODUCTION

Many studies have been conducted on the modelling and analysis of piezoelectric materials and structures. The early results were summarised by Rogacheva [1] and Tzou [2] in their books. Literature sources on the intelligent controlled structures are rich (Tani *et al*. [3], Stammers *et al.* [4], Sireteanu [5], Giuclea *et al*. [6], Mihailescu and Chiroiu [7], Chiroiu *et al*. [8]). Qiu *et al*. [9] has used a piezoelectric layer to suppress the static bending deformation of a composite plate with a temperature gradient in the thickness direction. Young and Hansen [10] studied the active control of flexural wave propagation in a beam terminated with arbitrary end conditions by using a piezoelectric stack actuator placed between a stiffener flange and the beam.

Piezoelectric fibre composites and ferroelectric materials have recently been introduced to address the issues of strength, conformability and manufacturability. Ferroelectric materials have multifunctional properties such a piezoelectricity, non-volatile charge, and electro-optic functions. Also, the shape memory piezoelectric actuator can be operated using a pulsed voltage, so that small energy consumption and small voltage operation can be realized (Morita *et al.* [11])

In this paper we propose a configuration for a semi-infinite strip with a piezoelectric layer which controls the displacements caused by mechanical loads. The piezoelectric material with Cantor-like structure is used as a distributed actuator, which can elongate or contract under externally applied voltage. When the main material elongates under external forces, voltage is applied on the Cantor-like structure of the piezoelectrics, so that it will elongate by the same length to

Institute of Solid Mechanics of the Romanian Academy, Bucharest, E-mail: veturiachiroiu@yahoo.com

Rev. Roum. Sci. Techn. – Méc. Appl., Tome 55, Nº 1, P. 51–62, Bucarest, 2010

cancel the bending deformation. The voltage sign is reversed if the main material contracts. Based on this principle, we show that the displacement distribution can be controlled actively by applying a voltage to the piezoelectric material.

2. THE THEORY

The stresses in a semi-infinite strip have been investigated theoretically by many authors (Theocaris [12], Ling and Cheng [13], Badea *et al.* [14]). In this work the semi-infinite strip is composed of two layers (Fig. 1): one layer made from a traditional material (M) of width $h_m = 2$cm, and another layer made from the piezoelectric material with Cantor-like structure (CM) of width $h = 0.2$cm. The later layer is used to control actively the bending deformation. The Cantor-like layer is formed by alternating elements of isotropic piezoelectric ceramics (PZ) and epoxy resin (ER), following a triadic Cantor sequence (Chiroiu *et al*. [15], Crăciun *et al*.[16] and Alippi *et al*. [17]). We use a triadic Cantor sequence up to the ∞ generation. The structure is bounded in the right half-plane $x \geq 0$ by the lines $x = 0$ and $y = 1$, $y = -1.2$. The strip is measured by a typical length l. The governing equations are

$$(t_{ij} + u_{k,i}\, t_{kj})_{,j} = 0, \tag{1}$$

$$D_{i,i} = 0, \; E_i + \varphi_{,i} = 0, \; i, j = 1, 2, \tag{2}$$

where u_i are the components of the displacement vector, t_{ij} are the components of the stress tensor, D_i of the electric induction vector, E_i of the electric field and φ is the electric potential. In the M and ER materials $\varphi = 0$. The constitutive equations of M, PZ and ER materials are (Kapelewski and Michalec [18])

$$\begin{aligned}
t_{ij} &= \lambda^m \varepsilon_{kk}\delta_{ij} + 2\mu^m \varepsilon_{ij} + A^m \varepsilon_{il}\varepsilon_{jl} + 3B^m \varepsilon_{kk}\varepsilon_{ij} + C^m \varepsilon_{kk}^2 \delta_{ij}, \\
t_{ij} &= \lambda^p \varepsilon_{kk}\delta_{ij} + 2\mu^p \varepsilon_{ij} + A^p \varepsilon_{il}\varepsilon_{jl} + 3B^p \varepsilon_{kk}\varepsilon_{ij} + C^p \varepsilon_{kk}^2 \delta_{ij} - \\
&\quad - e_k^p E_k \delta_{ij} - \overline{e}_k^p E_k \varepsilon_{ll}\delta_{ij} - \overline{\overline{e}}_k^p E_k \varepsilon_{ll}\delta_{ij} - \overline{\overline{e}}_k^p E_k \varepsilon_{ij}, \\
t_{ij} &= \lambda e^e \varepsilon_{kk}\delta_{ij} + 2\mu^e \varepsilon_{ij} + A^e \varepsilon_{il}\varepsilon_{jl} + 3B^e \varepsilon_{kk}\varepsilon_{ij} + C^e \varepsilon_{kk}^2 \delta_{ij}, \\
D_i &= \overline{\varepsilon}^p E_i - \frac{1}{2}\overline{\varepsilon}_i^p E^2 - e_i^p \varepsilon_{kk} - \frac{1}{2}\overline{e}_i^p \varepsilon_{kk}^2 - \frac{1}{2}\overline{\overline{e}}_i^p \varepsilon_{kl}^2, \\
\varepsilon_{ij} &= \frac{1}{2}(u_{i,j} + u_{j,i} + u_{l,i}u_{l,j}),
\end{aligned} \tag{3}$$

where ε_{ij} are the components of the strain tensor, λ, μ are the Lame constants (the indices m, p or e refer to M, PZ or ER materials), A, B, C are the Landau constants, $\overline{\varepsilon}^p, \overline{\varepsilon}_i^p$ ($\overline{\varepsilon}_3^p = \overline{\varepsilon}_2^p = \overline{\varepsilon}_1^p$) are the linear and nonlinear dielectric constants, e_i^p ($e_1^p = e_2^p = e_3^p$), $\overline{e}_i^p$ ($\overline{e}_1^p = \overline{e}_2^p = \overline{e}_3^p$) and $\overline{\overline{e}}_i^p$ ($\overline{\overline{e}}_1^p = \overline{\overline{e}}_2^p = \overline{\overline{e}}_3^p$) are the linear and nonlinear coefficients of piezoelectricity and $E^2 = E_1^2 + E_2^2 + E_3^2$. The equations (1)-(3) are nonlinear. Details on the simulation of the wave motion in nonlinear media can be found in Scalerandi *et al.* [19] and Chiroiu *et al.* [20].

We have

$$u_1 = u_1(x, y), \quad u_2 = u_2(x, y), \quad E_i = -\varphi_{,i}, \quad \varphi = \varphi(x, y), \quad i = 1, 2. \tag{4}$$

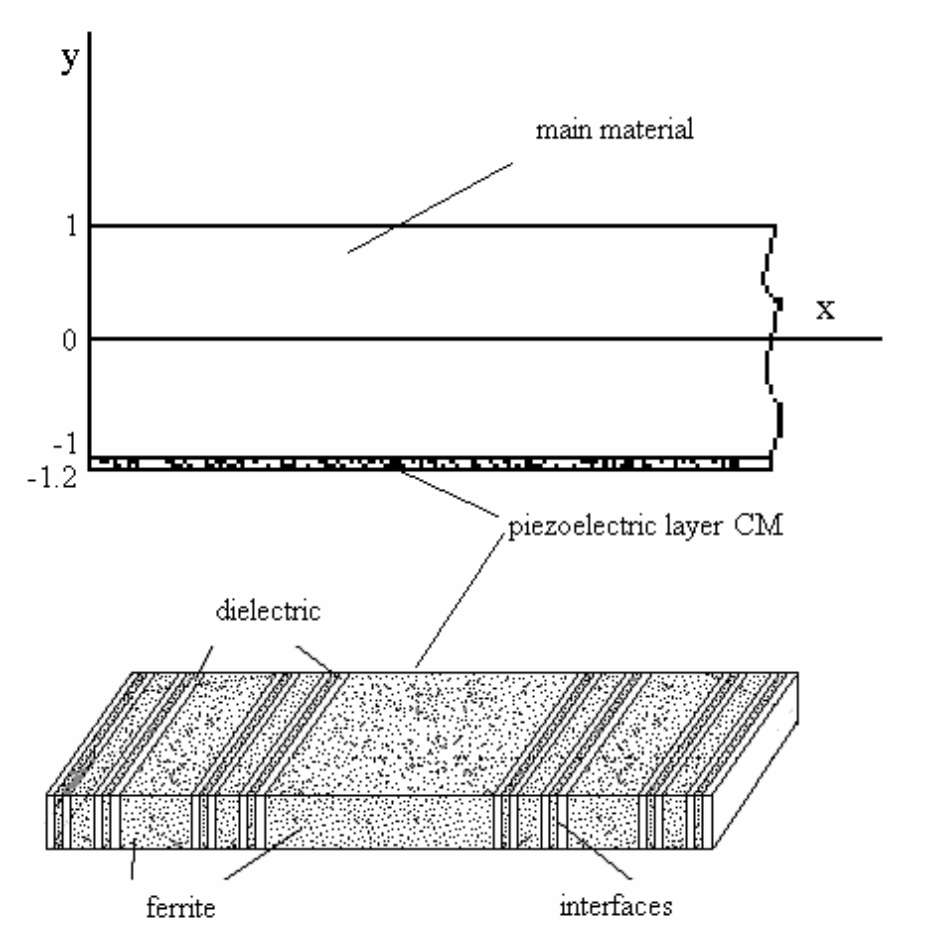

Fig. 1 – Configuration of the strip.

The boundary conditions are given by

$$t_{11}\big|_{x=0} = \overline{t}_{11} = \sum_{n=0}^{\infty} b_n \cos n\pi y\,, \quad t_{12}\big|_{x=0} = \overline{t}_{12} = \sum_{n=1}^{\infty} c_n \sin n\pi y\,, \tag{5}$$

for the traction along the transverse edge $x = 0$ and $-1 \le y \le 1$,

$$t_{22}\big|_{y=1} = F_1(x)\,, \quad t_{12}\big|_{y=1} = F_2(x)\,, \tag{6}$$

for the traction along the longitudinal edge $y = 1$ and $0 \le x < \infty$, and

$$[u_i] = 0\,, \quad [t_{22}] = [t_{12}] = 0\,, \quad i = 1,2\,, \tag{7}$$

for the continuity conditions on the interfaces between PZ and ER constituents (I^{pe}), where the bracket indicates a jump across the interface.

3. THE RITZ METHOD

Let us suppose that $S = \{u_1\,, u_2, \varphi\}$ are cubic functions of y (Frederiksen [20])

$$S_i(x,y) = \Psi_i(x)y + \Phi_i(x)y^2 + \Sigma_i(x)y^3\,, \quad i = 1,2,3\,, \tag{8}$$

where Ψ, Φ, Σ are unknown functions. Following the Ritz procedure, we assume the solution for Ψ, Φ, Σ to be in the form of finite series with unknown coefficients

$$\Psi_i(x) = \sum_{m}^{N} X_{im} w_m\left(\frac{x}{l}\right), \quad \Phi_i(x) = \sum_{m}^{N} Y_{im} w_m\left(\frac{x}{l}\right), \tag{9}$$

where $w_m(\varepsilon), -1 \le \varepsilon \le 1$ the degenerated beam functions defined for the dimensionless variable ε

$$\begin{aligned}
&w_0(\varepsilon) = 1\,,\ w_1(\varepsilon) = \varepsilon\,,\ w_m(\varepsilon) = \cos k_I\varepsilon\,,\ I = \frac{m+2}{2}\,, && m = 2,6,10,...\\
&w_m(\varepsilon) = \cosh k_J\varepsilon\,,\ J = \frac{m+1}{2}\,, && m = 3,7,11,...\\
&w_m(\varepsilon) = \sin k_I\varepsilon\,,\ I = \frac{m+2}{2}\,, && m = 4,8,12,...\\
&w_m(\varepsilon) = \sinh k_J\varepsilon\,,\ J = \frac{m+1}{2}\,, && m = 5,9,13,...
\end{aligned} \tag{10}$$

where k_m is the solution of the equation

$$\tan k_m + (-1)^m \tanh k_m = 0\,, \quad m = 2,3,4,\ldots\,. \tag{11}$$

Though the functions (10) do not satisfy free edge conditions, it was shown that for problems involving free edges the series composed of these functions converge rapidly towards highly accurate solutions. The arbitrary coefficients X, Y, Z in the series (9) are determined from the stationary value of a classical functional

$$\begin{aligned} H &= \int_0^L \mathrm{d}x \left\{ \int_{-1.2}^{1} \bar{U}\mathrm{d}y \right\} + \int_{-1.}^{1} (t_{ij}\big|_{x=0} - \bar{t}_{ij}) n_j u_i \mathrm{d}y + \int_{0.}^{L} (t_{ij}\big|_{y=1} n_j - F_i) u_i \mathrm{d}x + \int_{I^{pe}} t_{ij} n_j u_i \mathrm{d}x\,, \\ \bar{U} &= -U + (t_{ij} + u_{k,i}\, t_{kj}) \left(\varepsilon_{ij} - \frac{1}{2} u_{i,j} - \frac{1}{2} u_{j,i} - u_{l,i}\, u_{l,j} \right) - D_i (E_i + \varphi_{,i})\,, \end{aligned} \tag{12}$$

where U is the internal energy

$$U = \frac{1}{2}\left[(t_{ij} + u_{k,i} t_{kj}) \varepsilon_{ij} + E_i D_i \right]. \tag{13}$$

4. RESULTS AND CONCLUSIONS

Consider four particular cases as shown in Fig. 2. In each case $F_1(x) = F_2(x) = 0$. In the case 1 the transverse edge of the strip is under a segment of uniform compressive load of p per unit length over a length $2c$ from $y = -c$ to $y = c$, $c \le 1$. The given boundary condition along $x = 0$ is

$$\begin{aligned} t_{11}\big|_{x=0} &= 0\,, \quad -1 \le y < c \text{ and } c < y \le 1\,, \\ t_{11}\big|_{x=0} &= -p\,, \quad -c \le y \le c\,. \end{aligned} \tag{14}$$

In the case 2, the transverse edge is under a pair of concentrated compressive loads of P each at the points $y = \pm c$. The boundary condition along $x = 0$ is

$$t_{11}\big|_{x=0} = -\frac{P}{l}\{\delta(y+c) + \delta(y-c)\}\,, \quad -1 \le y \le 1\,, \tag{15}$$

where $\delta(y)$ is the Dirac delta function.

In the case 3, the transverse edge is under a pair of concentrated tangential loads of Q each, directed away from each other, at the points $y = \pm c$. The boundary condition along $x = 0$ is

$$t_{12}\big|_{x=0} = \frac{Q}{l}\{\delta(y+c) - \delta(y-c)\}, \quad -1 \le y \le 1. \tag{16}$$

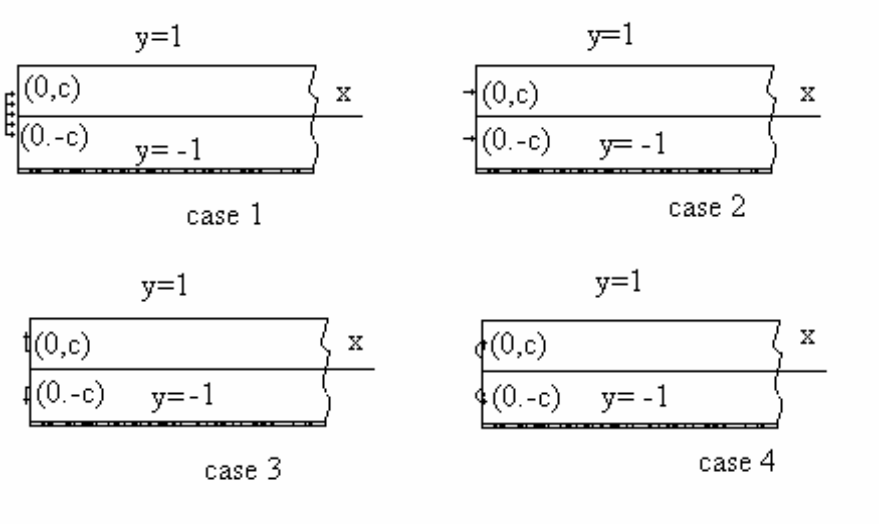

Fig. 2 – The loading cases.

In the case 4, the transverse edge is under a pair of equal and opposite couples at the points $y = \pm c$. The boundary condition can be derived from the case 2.

Table 1

The material constants

	copper	piezoelectric ceramics	epoxy resin
λ	119.9 GPa	71.6 GPa	42.31 GPa
μ	23.1 GPa	35.8 GPa	3.76 GPa
A	–351 GPa	–2,000 GPa	2.8 GPa
B	–60.5 GPa	–1,134 GPa	9.7 GPa
C	–103 GPa	–900 GPa	–5.7 GPa
$\overline{\varepsilon}$	–	4.065 nF/m	–
$\overline{\varepsilon}_1$	–	2.079 nF/m	–
e_1	–	–0.218 nm/V	–
$\overline{e}_1$	–	–0.435 nm/V	–
ρ	8,930 kg/m^3	7,650 kg/m^3	1,170 kg/m^3

Table 2

Normal stress $t_{11}\big|_{y=0}$ [GPa] and displacements u_1 and u_2 [mm] along x-axis for the case 1 ($c = 0.5$, $p = 1$)

x	$E = 0$ V/m	$E = 4\times10^7$ V/m	$E = 5\times10^7$ V/m	$E = 6.2\times10^7$ V/m
0	–1.013 –1.002 –0.782	–1.045 –0.204 –0.666	–1.429 –0.056 –0.341	–1.545 –0.007 –0.012
0.25	–0.977 –0.982 –0.771	–1.248 –0.184 –0.373	–1.338 –0.043 –0.215	–1.574 –0.007 –0.010
0.5	–0.871 –0.656 –0.563	–0.945 –0.143 –0.231	–1.243 –0.035 –0.200	–1.444 –0.006 –0.010
1	–0.655 –0.545 –0.432	–0.743 –0.107 –0.108	–0.966 –0.027 –0.124	–1.421 –0.005 –0.009
2	–0.521 –0.470 –0.381	–0.840 –0.083 –0.094	–0.979 –0.019 –0.117	–1.365 –0.004 –0.008
3	–0.499 –0.370 –0.276	–0.644 –0.057 –0.066	–0.857 –0.016 –0.054	–0.978 0 –0.003
5	–0.514 –0.165 –0.144	–0.788 –0.014 –0.019	–1.167 –0.012 –0.032	–1.389 0 0
6	–0.501 –0.113 –0.109	–0.666 –0.010 –0.009	–1.044 –0.045 –0.033	–1.130 0 0
∞	–0.500 –0.034 –0.013	–0.677 –0.008 –0.002	–1.055 –0.006 0	–1.145 0 0

Consider the transverse edge be under a pair of normal concentrated loads of $-P$ each at the points $y = \pm c$ and a second pair of normal concentrated loads of P each at $y = \pm(c + \Delta c)$. Denote the couple $C = Pl\Delta c$. For $P \to \infty$, $\Delta c \to 0$, C tends to a finite quantity. The material constants are shown in table 1.

The variation of normal stresses $t_{11}\big|_{y=0}$ or $t_{22}\big|_{y=0}$ [GPa] and the displacements u_1 and u_2 [mm] along x-axis for each case are illustrated in tables 2–5 (in each place the first row is the stress and then u_1 and u_2). In order to reduce the displacement field, electric field $E_2 = E$ is applied to piezoelectric material in

the y direction. When the electric field is applied the displacement field decreases. As the tables show for $E = 6.2 \times 10^7$ V/m the displacements are almost cancelled.

Table 3

The normal stress $t_{11}\big|_{y=0}$ [GPa] and displacements u_1 and u_2 [mm] along x-axis for the case 2 ($c = 0.5$, $P/l = 1$)

x	$E = 0$ V/m	$E = 4 \times 10^7$ V/m	$E = 5 \times 10^7$ V/m	$E = 6.2 \times 10^7$ V/m
0	0	–0.123	–0.317	–0.561
	0	–0.002	–0.001	0
	0	–0.011	0	0
0.25	–0.232	–0.343	–0.793	–0.968
	–0.277	–0.023	–0.003	0
	–0.218	–0.019	–0.002	0
0.5	–0.715	–0.767	–0.881	–0.996
	–0.355	–0.028	–0.007	0
	–0.247	–0.029	–0.004	0
1	–1.012	–1.314	–1.484	–1.502
	–0.499	–0.089	–0.009	0
	–0.270	–0.033	–0.006	0
2	–1.004	–1.250	–1.299	–1.328
	–0.504	–0.109	–0.010	0
	–0.344	–0.038	–0.007	0
3	–0.999	–1.129	–1.324	–1.428
	–0.560	–0.166	–0.020	0
	–0.355	–0.050	–0.049	0
5	–1.004	–1.245	–1.376	–1.459
	–0.657	–0.197	–0.037	–0.003
	–0.444	–0.073	–0.125	–0.001
6	–1.000	–1.245	–1.497	–1.555
	–0.713	–0.229	–0.047	–0.004
	–0.562	–0.149	–0.114	–0.002
∞	–1.000	–1.245	–1.497	–1.654
	–0.887	–0.398	–0.060	–0.004
	–0.699	–0.270	–0.146	–0.002

When no electric field is applied, in the first case the maximum displacement is $u_{\max} = u_1 = 1.002$ mm at $x = 0$. This displacement is reduced to 0.056 mm when $E = 5 \times 10^7$ V/m, and respectively to 0.007 mm when $E = 6.2 \times 10^7$ V/m. In the second case $u_{\max} = u_1 = 0.887$ mm at $x = \infty$ and is reduced to 0.060 mm and respectively to 0.004 mm. In the third case $u_{\max} = u_2 = 1.183$ mm at $x = 0$ and is reduced to 0.120 mm and respectively 0.002 mm. In the last case

$u_{\max} = u_2 = 1.054$ mm at $x = 0$ and is reduced to 0.133 mm and respectively, 0.003 mm.

Table 4

The normal stress $t_{22}\big|_{y=0}$ [GPa] and displacements u_1 and u_2 [mm] along x-axis for the case 3 ($c = 0.5$, $Q/l = 1$)

x	$E = 0$ V/m	$E = 4\times10^7$ V/m	$E = 5\times10^7$ V/m	$E = 6.2\times10^7$ V/m
0	3.319 1.166 1.183	3.987 0.123 0.130	4.717 0.102 0.120	5.087 0.002 0.002
0.25	2.099 1.122 1.168	2.454 0.113 0.089	2.093 0.100 0.116	2.183 0.002 0.001
0.5	0.776 0.797 0.867	0.971 0.105 0.044	1.251 0.043 0.109	1.447 0.001 0.001
1	–0.081 0.514 0.547	–0.194 0.069 0.023	–0.364 0.034 –0.034	0.567 –0.001 0
2	–0.079 –0.354 –0.408	–0.249 –0.028 –0.019	–0.477 –0.019 –0.028	–0.657 0 0
3	–0.009 –0.255 –0.405	–0.106 –0.021 –0.014	–0.379 –0.018 –0.023	–0.445 0 0
5	–0.007 –0.144 –0.202	–0.065 –0.009 –0.010	–0.237 –0.015 –0.019	–0.463 0 0
6	–0.001 –0.009 –0.018	–0.004 –0.002 –0.007	–0.020 –0.011 –0.008	–0.044 0 0
∞	0 0 0	0 0 0	0 0 0	0 0 0

When the electric field is applied the stress increases. We note that the stress in material is under the material strength when electric field is $E = 6.2\times10^7$ V/m.

In conclusion, the application examples show that this configuration can successfully cancel the displacements cased by external mechanical loads.

The normal stress $t_{11}|_{y=0}$ [GPa] along x-axis for the case 2 ($c=0.5$, $P/l=1$) in the main layer of the strip and respectively, the piezoelectric layer is represented in Fig. 3, for $E=6.2\times10^7$ V/m.

The analysis of the relationship between the electric field and displacements mm] of the CM piezoelectric layer, a good linearity and non-hysteresis in behaviour performance is obtained (Fig. 4).

Table 5

Normal stress $t_{22}\big|_{y=0}$ [GPa] along x-axis for the case 4 ($c=0.5$, $C/L^2=1$)

x	$E=0$ V/m	$E=4\times10^7$ V/m	$E=5\times10^7$ V/m	$E=6.2\times10^7$ V/m
0	1.211	1.333	1.356	1.546
	1.044	0.166	0.123	0.002
	1.054	0.175	0.133	0.003
0.25	2.609	2.778	2.989	3.128
	0.968	0.145	0.119	0.002
	0.999	0.166	0.121	0.002
0.5	0.111	0.256	0.599	0.679
	0.768	0.122	0.045	0.001
	0.822	0.145	0.066	0.002
1	–0.912	–1.342	–1.593	–1.987
	0.056	0.008	–0.012	0
	0.099	0.009	–0.044	0
2	–0.232	–0.432	–0.529	–0.770
	–0.178	–0.013	–0.008	0
	–0.199	–0.033	–0.034	0
3	–0.019	–0.258	–0.299	–0.435
	–0.256	–0.009	–0.007	0
	–0.211	–0.021	–0.013	0
5	–0.005	–0.015	–0.022	–0.134
	–0.145	–0.008	–0.005	0
	–0.188	–0.013	–0.007	0
6	–0.003	–0.005	–0.009	–0.012
	–0.123	–0.007	–0.001	0
	–0.145	–0.009	–0.001	0
∞	0	0	0	0
	0	0	0	0
	0	0	0	0

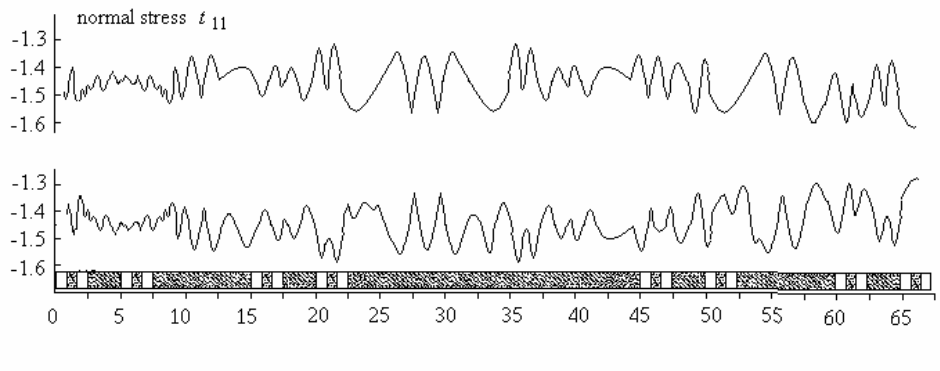

Fig. 3 – The normal stress $t_{11}\big|_{y=0}$ along x-axis, case 2 ($c = 0.5$, $P/l = 1$) in both layers.

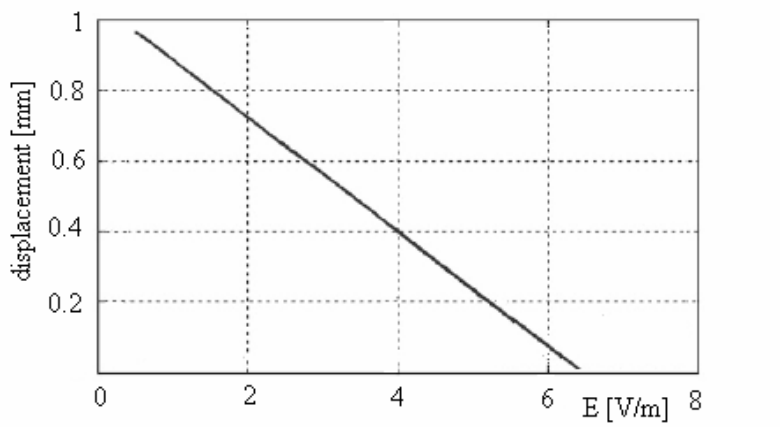

Fig. 4 – The relationship between the electric field and displacement of the CM layers.

Acknowledgments. The authors gratefully acknowledge the financial support of the National Authority for Scientific Research (ANCS, UEFISCSU), through PN-II research project no. 106/2007, code ID_247/2007, and the National Centre for Programme Management (CNMP) through PNCDI-II-P4 research project no. 81031/2007.

Received on March 17, 2010

REFERENCES

1. ROGACHEVA, N.N., *The theory of piezoelectric shells and plates*, CRC Press, Boca Raton, 1993.
2. TZOU, H. S., *Piezoelectric shells*, Kluwer Acad. Publ., 1993.
3. TANI, J., TAKAGI, T., QIU, J., *Intelligent material systems: Application of functional materials*, ASME Appl. Mech. Rev., **51**, *8*, pp. 505-521, 1998.

4. STAMMERS, C.W., URSU, I., URSU, T., SIRETEANU, T., *Artificial intelligence based synthesis of semi-active suspension systems,* Shock & Vibration Digest, **32**, *1*, pp. 2-10, 2000.
5. SIRETEANU, T., GHIȚĂ, Gh., STĂNCIOIU, D., *Fluide şi amortizoare magneto-reologice*, Edit. Bren, Bucharest, 2005.
6. GIUCLEA, M., SIRETEANU, T., GHIȚĂ, Gh., *Metode de inteligență computațională cu aplicații la sisteme dinamice*, Edit. Bren, Bucharest, 2009.
7. MIHAILESCU, M., CHIROIU, V., *Advanced mechanics on shells and intelligent structures*, Edit. Academiei, Bucharest, 2004.
8. CHIROIU, V., MIHAILESCU, M., MUNTEANU, L., *Applications of smart materials in engineering*, Chap. 3, in: *Advanced Engineering in Applied Mechanics* (eds. T. Sireteanu, L. Vlădăreanu), Edit. Academiei, Bucharest, pp. 77-107, 2006.
9. QIU, J., TANI, J., TAKAGI, T., *An inteligent piezoelectric composite material without bending deformatiom*, Journal of Technical Physics, **35**, *1-2*, pp. 99-107, 1994.
10. YOUNG, A.J., HANSEN, C.H., *Control of flexural vibration in a beam using a piezoelectric actuator and an angle stiffener*, Journal of the Intelligent Material Systems and Structures, **5**, *4*, pp. 536-549, 1994.
11. MORITA, T., KADOTA, Y., HOSAKA, H., *Shape memory piezoelectric actuator*, Applied Physics Letters, **90**, 082909, 2007.
12. THEOCARIS, P.S., *The Concept of Mesophase in Composites*, Springer-Verlag, 1987.
13. LING, C.-B., CHENG, F.-H., *Stresses in a semi-infinite strip*, Int. J. Engng. Sci., **5**, *2*, pp. 155-179, 1967.
14. BADEA, T., CHIROIU, V., MUNTEANU, L., *The active control of motion in a composite structure*, ASME-IMECE, Active Control of Noise and Vibration, **305**, pp. 711-719, 2001.
15. CHIROIU, C., DELSANTO, P.P., SCALERANDI, M., CHIROIU, V., SIRETEANU, T., S*ubharmonic generation in piezoelectrics with Cantor-like structure,* Journal of Physics D: Applied Physics, **34**, *3*, pp. 1579-1586, 2001.
16. CRACIUN, F., BETTUCCI, A., MOLINARI, E., PETRI, A., ALIPPI, A., *Direct experimental observation of fracton mode patterns in one-dimensional Cantor composites*, Phys. Rev. Lett., **68**, *10*, pp. 1555-1558, 1992.
17. ALIPPI, A., SHKERDIN, G., BETTUCCI, A., CRACIUN, F., MOLINARI, E., PETRI, A., *Threshold lowering for subharmonic generation in Cantor-like composite structures*, Physica A: Statistical Mechanics and its Applications, **191**, *1-4*, pp. 540-544, 1992.
18. KAPELEWSKI, J., MICHALEC, J., *Soliton-like SAW in nonlinear isotropic piezoelectrics*, Int. J. Engng. Sci., **29**, *3*, pp. 285-291, 1991.
19. SCALERANDI, M., DELSANTO, P.P., CHIROIU, C., CHIROIU, V., *Numerical simulation of pulse propagation in nonlinear 1-D media*, Journal of the Acoustical Society of America, **106**, pp. 2424-2430, 1999.
20. CHIROIU, V., CHIROIU, C., RUGINĂ, C., DELSANTO, P.P., SCALERANDI, M., *Propagation of ultrasonic waves in nonlinear multilayered media,* Journal of Computational Acoustics, **9**, *4*, pp. 1633-1646, 2001.
21. FREDERIKSEN, P.S., *Identification of Material Parameters in Anisotropic Plates- A combined numerical/experimental method*, Ph.D. Thesis, Dept. of Solid Mechanics, The Technical University of Denmark, 1992.